COMPUTING TURBULENT FLOW FIELD OF SWIRL JET

Nabil H. Mostafa
Mechanical Power Department, College of Engineering
Zagazig University, Zagazig, 44519, Egypt.
E-mail: nmostafa@vt.edu

حساب الإضطراب في مجال السريان لنفث حلزونى

نبيل حسن مصطفى
قسم هندسه القوى الميكانيكيه. كليه الهندسه
جامعه الزقازيق- الزقازيق ٤٤٥١٩ – مصر

خلاصه

لقد تم حساب الإضطراب لنفث حر يتعرض للإثاره من مائع و كذلك تأثيره على تطور انتشار النفث. فقد تم تعريض النفث الحر لنفاثات مولده للدوامات وضعت قرب مخرج المنفث الرئيسى لتوليد نفث حلزونى. وكان رقم رينولد ١٧٠٠٠ للمنفث الرئيسى و كانت نسبه كميه التحرك بين النفاثات المولده للدوامات و النفث الرئيسى تتراوح بين ٥,٥ و ٧,٨ و ٩,٥ و ٢٨,٥ % و كان ذلك مع تغيير نسبه السرعه بين النفاثات المولده للدوامات و النفث الرئيسى حتى التساوى. وكان حقن النفاثات المولده للدوامات يتم مماسيا و مائلا بزاويه ٤٥ و ٩٠ درجه بالنسبه للنفث الرئيسى.

إن ديناميكيه انتشار النفث الحلزونى قد حسبت باستعمال برنامج حسابى لحل معادلات نافير استوكس فى ثلاث اتجاهات و المسمى (CFDRC 2000) . يتم تمثيل المعادلات الحاكمه على شبكه منشأه باستخدام نظام فرق الاختلاف المضاد للاتجاه. أن التركيب العام لمنظر النفث الحلزونى قد توقش مع الأضطراب فى الضغط و السرعه. و كذلك قورن إنتشار النفث الحلزونى النفث الغير مثار.

أن استخدام نفاثات مولده للدوامات نتج عنه زياده الخلط بين النفث المضطرب و المائع المحيط و مع امكانيه التحكم فى منظر النفث. أن استخدام النفاثات المولده للدوامات يزيد زاويه انتشار النفث عن حاله النفث غير المثار. أن النفث الحلزونى ذو الحقن بزاويه ٤٥ درجه مع أعلى نسبه كميه تحرك يعطى أعلى طاقه أضطراب عن النفث غير المثار بنسب ١٨,٥% و ٢٩,٤% و ٣٨,٧% و ١٢٢,٦% و ذلك لنسب كميه تحرك ٥,٥ و ٧,٨ و ٩,٥ و ٢٨,٦ % على التتابع. أن النفث الحلزونى يعطى اجهادات مرتفعه فى منطقه اسطوانيه ذو قطر يساوى ٨. من قطر المنفث وعلى ارتفاع يقدر من ٢ الى ٣ أقطار المنفث متوقفا على نسبه الاندفاع. إن النتائج الحسابيه قد قورنت بالنتائج العمليه السابق اجرائها بواسطه مجس السلك الساخن ذو اربعه اسلاك و السابق نشرها بواسطه الباحث (٢٠٠٠) أن النتائج أوضحت الاتفاق الواضح بين النتائج المعمليه و النظريه.

ABSTRACT

A computing of a turbulent jet subjected to fluidic excitation and it's effect on the jet evolution was conducted. The jet was subjected to vortex generating jets placed at the exit of the main jet nozzle exit to generate Swirl Jet. The main jet had a R_{en} about 17000, and the VGJ to main jet momentum ratio were 0.055, 0.095, 0.078 and 0.285. The velocity ratio between the VGJs and main jet ($CR = C_{vgj}/C_{jet}$) was varied up to unity. The activation of VGJ was tangential (α=0), (α=45 degree) and (α=90 degree).

In non-reacting Swirl Jets, the dynamics of the flow field structure were computed using a three-dimensional Navier-Stokes code (CFDRC, 2000). The governing equations are discretized on a structured grid using an upwind difference scheme. The macroscopic

Accepted June 18, 2001

behaviour of the jet evolution is discussed with the turbulent pressure and velocities. The transport of jet fluid is compared with the unexcited jet.

The use of Vortex Generator Jets to enhance the mixing between a turbulent jet and the surrounding fluid is shown to offer improvement and control over the jet evolution. VGJ's enhance the jet spreading angle over unexcited jet. The Swirl Jet with injection angle (α=45) and the higher momentum injection gives maximum higher Turbulent Kinematics Energy than the Baseline Jet by 18.5, 29.4, 38.7 or 122.6% for momentum ratios equal 0.055, 0.078, 0.095 and 0.285 respectively. With Swirl Jet excitation the high stress region located at a cylinder layer of diameter 0.8 of nozzle diameter and moving horizontally in a section from 2 to 3 z/D from upstream according to momentum ratio. These computational data are compared with the experimental results obtained with a four-wire hot-wire velocity probe by the author (Mostafa, 2000). The results show great agreement with the experimental results at different conditions of Swirl Jet flow.

KEYWORDS
Swirl Jet, Vortex Generating Jets, CFD, Turbulent.

NOMENCLATURE

C_{jet} mean velocity of main jet (m/s).
C_{vgj} mean velocity of VGJ jet (m/s).
C_R ratio of the VGJ velocity to the main jet velocity (not including injection flow).
$C_\mu, C_\varepsilon, C_\kappa$ constants
d_{vgj} diameter of the VGJ nozzle (mm).
d_{jet} diameter of main jet nozzle (mm).
κ turbulence kinetic energy (m^2/s^2)
mr momentum ratio of the flow of the VGJs to the main jet flow momentum.
r, t local polar, radial and tangential coordinates, respectively.
r_o, t_o main polar, radial and tangential, coordinates, respectively.
R_{en} Reynold number.
U axial velocity, (m/s).
u' turbulence fluctuation component of axial velocity, (m/s).
V horizontal velocity component in r-axis, (m/s).
v' turbulence fluctuation component of V velocity, (m/s).
v_t turbulent viscosity
W the horizontal velocity component in the direction of t_o-axis, (m/s).
w' turbulence fluctuation component of W velocity, (m/s).
z Axial coordinate.

GREEK LETTERS

α angle of VGJ injector axis relative to tangent of nozzle cross section in degrees.
β angle between VGJ axis and main jet axis in degrees.
ρ density, (Kg/m^3).
θ jet total spreading angle in degrees.
$\sigma_k, \sigma_\varepsilon$ constants
μ dynamic viscosity (pa.s)
ε turbulence dissipation rate (J/Kg.s)

SUFFIXES

jet main jet
vgj vortex generator jet

ABBREVIATIONS

PSJ Pulsed Swirl Jet generated from the interaction between pulsed injection of VGJs with a free jet.

SJ Swirl Jet generated from the interaction between continuous injection of VGJs with a free jet.

VGJ Vortex Generator Jet.

1- INTRODUCTION

Flow in free shear flows like jets and mixing layers are characterized by vortex formation. In these regions, the turbulence intensity is very high. These structures play in controlling the mixing between two fluid streams. Turbulence scales results from strong pressure fluctuations on the mixing layer or the jet exit.

Over the past two decades studies were conducted on the effect of vortex dynamics on jet flow evolution. Controlling the jet evolution can be obtained by passive and active methods. Passive methods are limited for certain performanee like using vortex ring which were analyzed by Martin and Meiburg (1991). Also, Using small tabs at nozzle exit, Zaman and et al., (1994), or crown shaped nozzles, Longmire et al (1992), which was limited by the number and length of the crown teeth. Corke and Kusek (1993) discussed active control of fundamental two-and three dimensional amplified modes in an axisymmetric jet by introducing localized acoustic disturbances produced by an azimuthal array of miniature speakers placed close to the jet lip on the exit face. Husain and Hussain (1993) discussed the dynamics of the preferred mode coherent structure in the near field of elliptic jets. They also addressed the effect of initial conditions and excitation frequency and amplitude on the elliptic jet instability and its evolution.

Although convenient and easy to use, acoustic drivers are mostly not suitable for controlling flows of practical interest. Among the many reasons which can be cited are lack of space for installation, loss of effectiveness in noisy environments like combustors and possible reliability problems. Alternative active methods have been also examined, these included mainly mechanically vibrating elements at the jet exit. Piezoelectric actuators were used to excite free shear flows for square jet by Wiltse and Glezer (1993). Vandsburger and Ding (1995) examined a triangular nozzle fitted with mechanically amplified piezoceramic actuators on all three sides. For the purpose of achieving control over the jet evolution into the far field (L/D = 30) various azimulthal (spatial) modes were excited. It was found that fractional spatial modes (e.g. m = 0.75) and wave combinations (e.g. m = ± 0.5) offered the best jet mixing control.

In spite of the wealth of data available, industry shies away from using moving parts as flow actuators. Therefore, a practical excitation device should have minimum power consumption and no moving parts, while producing an excitation that is controllable in frequency, amplitude and phase. The possibility exists for employing fluid jet actuators. The viability and performance of an unsteady fluid-dynamic excitation system was examined by Raman and Cornelius (1995) for the control of turbulent jets. They demonstrated that a jet flow could be forced by two miniature fluidic exciter jets. This technique produced very large velocity perturbations in the main jet. The application of fluid based actuators to subsonic jets has been examined in recent years by the group of Glezer at Georgia Tech using "synthetic jets" (Parekh et al 1996). These actuators add no mass, but do add momentum for actuation to the excited jet.

The evolution of a free round jet using vortex generating jets placed around the main jet nozzle exit (named Swirl Jet) was experimentally discussed by the authors previously, Mostafa and et al. (1995). Activation of the VGJs resulted in enhanced mixing

of the jet fluid and the ambient fluid. The activation of tangential (α=0) VGJs in a pulsed manner enhanced the main jet spreading over continuous VGJs in non-reacting and reacting PSJ, which were experimentally discussed by Mostafa et al. (1996) and Mostafa and Vandsburger (1998), respectively. The mean flow is defined by a simple average over 1008 samples each measuring point using a four-wire hot-wire velocity probe. Mean velocity components (U, V, W) for the baseline jet and a jet subjected to VGJs at (α =0°, mr= 0.055), (α =45°, mr= 0.055), (α=0°, mr= 0.078) and (α =45°, mr= 0.078), are compared by Mostafa et al (1999). All VGJs exited cases show a better dispersion of the main jet fluid momentum as evidenced by smaller gradients of the isointensity contours for equivalent cross sections. The higher VGJs momentum case mr=0.078 exhibits higher dispersion than the mr=0.055 case. The effect of the VGJs on the level and distribution of the normal Reynolds stress is discussed by Mostafa (2000).

The objective of this paper is to compute the flowfield structure, turbulence generation and evolution in a swirl jet, "a free jet subjected to VGJs excitation". The present paper reports the modification to a turbulent jet due to the application of vortex generator jets (VGJs) in a continuous manner. The main parameters of the study is the angle of the VGJs with respect to the main jet, and the momentum ratio between the VGJs and the main jet. All fluids are assumed to be cold air.

2- THEORY BACKGROUND

The basic approach is to use standard viscous flow (Navier- Stokes) equations with provisions for variable density and a conventional turbulence model, such as K-ε model. A numerical model previously developed by CFDRC to solve (Navier- Stokes) equations (Sighal 1999).

The issue of turbulence modeling arises from the need to represent turbulent or Reynolds stresses, which are additional unknowns are introduced by averaging the Navier- Stokes equations. One common approach is the Eddy Viscosity Modeling (EVM) approach in which the Reynolds stress tensor is assumed to be proportional to the rate of mean strain, by analogy with the laminar stress- strain relationship. The proportionality parameter is called the turbulent or eddy viscosity. Unlike its laminar counter- part, the turbulent viscosity is not a property of the fluid but rather a characteristic of the flow. Several versions of the *k*- ε model are in use in the literature. They all involve solutions of transport equations for turbulent kinetic energy (*k*) and its rate of dissipation (ε). In the model, the turbulent viscosity is expressed as,

$$\nu_t = \frac{C_\mu k^2}{\varepsilon} \tag{1}$$

The transport equations for *k* and ε are,

$$\frac{\partial}{\partial t}(\rho k) + \frac{\partial}{\partial x_j}(\rho u_j k) = \rho P - \rho\varepsilon + \frac{\partial}{\partial x_j}[(\mu + \frac{\mu_t}{\sigma_k})\frac{\partial k}{\partial x_j}] \tag{2}$$

$$\frac{\partial}{\partial t}(\rho \varepsilon) + \frac{\partial}{\partial x_j}(\rho u_j \varepsilon) = C_{\varepsilon 1}\frac{\rho P \varepsilon}{k} - C_{\varepsilon 1}\frac{\rho \varepsilon^2}{k} + \frac{\partial}{\partial x_j}[(\mu + \frac{\mu_t}{\sigma_\varepsilon})\frac{\partial \varepsilon}{\partial x_j}] \tag{3}$$

where P is defined as

$$P = \nu_t(\frac{\partial u_i}{\partial x_j} + \frac{\partial u_i}{\partial x_j} - \frac{2}{3}\frac{\partial u_m}{\partial x_m}\delta_{ij})\frac{\partial u_i}{\partial x_j} - \frac{2}{3}k\frac{\partial u_m}{\partial x_m} \tag{4}$$

3- RESULTS AND DISCUSSION

The Swirl Jet flow analysis is computed for different momentum ratio of the VGJ flow to main jet flow. There are four sets of results that are computed for unexcited jet (baseline jet) and Swirl Jet at different injection angles (α=0, 45, 90 degrees).

The Swirl Jet structure is shown in figure 1a. The structure grids are divided into four reetangular faces revolved 360°. This uses the multiblock system. Three of them at the nozzle each have 5x5x40 grid points and one downstream 60x50x40 grid points. The grids are clustered near the VGJ to solve the fluid interaction. The length of the grid in physical domain is about $21d_{jet}$ length and $10d_{jet}$ diameter as shown in figures 1b and 1c.

3.1- MEAN FLOW ANALYSIS

Mean velocity components (U, V, W) for the baseline jet and a jet subjected to VGJs at momentum ratio (0.055, 0.078, 0.095 and 0.285), each of them injected at angles (α=0, 45 and 90). A comparison of the jet axial velocity component distribution across the main jet for the above thirteen conditions is shown in Figure 2. Due to the symmetry of the jet view, it is represented half the jet around Z-axis. All VGJs exited cases show a better dispersion of the main jet fluid, especially at α=45, as evidenced by smaller gradients of the iso-intensity contours for equivalent cross sections. The higher VGJs momentum case mr=0.285 exhibits higher dispersion than mr=0.095, mr=0.078 and mr=0.055 cases. The momentum ratio 0.285 is equivalent to CR equal unity. Figure 3 represents the iso-contour horizontal velocity component in r-axis for baseline jet and Swirl Jet across, α=45°, diametric plane. Thc higher VGJs momentum case mr=0.285 exhibits higher horizontal velocity component than baseline jet and Swirl Jet with lower momentum ratio cases. Iso-contours of the horizontal velocity component in the direction of t_o-axis in a horizontal plane at z/D=0 for the above three jets conditions are shown in Figure 4. The maximum magnitude of this component is, also, associated with maximum injection momentum ratio.

3.2: TURBULENCE STRESSES

A primary objective of this paper is to study the turbulence production mechanisms in the Swirl Jet. The turbulence characteristics of the baseline and excited jets were obtained as turbulent kinetic energy (k) and its rate of dissipation (ε).

Isovalue contour plots of turbulent rate of dissipation (ε) in a vertical diametric plane are shown in figure 5, for the baseline jet and a jet subjected to VGJs at momentum ratio (0.055, 0.078, 0.095 and 0.285), each of them injected at angles (α=0, 45 and 90). The maximum value of (ε) in the above thirteen conditions are 7320, (7332, 8675, 8879), (7328, 9470, 8879), (7324, 10150, 9297), (11301, 16299, and 20518) J/Kg.s, respectively as shown in figure 2. Thc increase of maximum turbulent dissipation rate in the Swirl Jet relative to a baseline jet (ε_{Sj} - ε)/ ε, is found to be (0.16, 18.5, 21.2), (0.1, 29.4, 21.3), (.05, 38.7, 27), (54.4, 122.6, 180.3) %.

The Swirl Jet Turbulent Kinematics Energy, (k), map are presented into two dimensional iso-value contour. Axial contour map of the Turbulent Kinematics Energy for the baseline jet and a jet subjected to VGJ at (α=0°, mr=0.055), (α=45°, mr=0.055), (α=90°, mr=0.055), (α=0°, mr=0.078), (α=45°, mr=0.078), and (α=90°, mr=0.078), are shown in figures 6.a, b, c, d, e, f, and g, respectively. All VGJs excited cases show higher Turbulent Kinematics Energy than the Baseline Jet. The higher VGJs momentum case mr=0.078 exhibits higher Turbulent Kinematics Energy than the case mr=0.055. With excitation the high stress region located at a cylinder layer of diameter 0.8 of nozzle diameter parallel to nozzle wall and at horizontal section of 2-3 z/D from upstream.

As a comparison with experimental data using hot wire probe, Mostafa (2000), the Swirl Jet Total Turbulent Kinematics Energy, TTKE ($U'^2+ V'^2+W'^2$), map are presented into two dimensional iso-value contour. Axial contour map of the TTKE for the baseline

jet and a jet subjected to VGJ at (α=0°, mr=0.055), (α=45°, mr=0.055), (α=0°, mr=0.078) and (α=45°, mr=0.078), are shown in figures 7.a, b, c, d, e respectively. All VGJs excited cases show higher Turbulent Kinematics Energy than the Baseline Jet. The higher VGJs momentum case mr=0.078 exhibits higher Turbulent Kinematics Energy than the case mr=0.055. With Swirl Jet excitation the high stress region located at a cylinder layer of diameter 0.8 of nozzle diameter and at horizontal section of 2.2 z/D from upstream which is completely matched with the theoretical results. Tangential VGJs injection des not similar to experimental results since the experimental results does not allow ideal tangentional injection (Non-radial component) because it have $\pm$ 8 degrees deviation due to the diameter of VGJ.

The Swirl Jet Turbulent Kinematics Energy, (k), map are presented into two dimensional iso-value contour. Axial contour map of the Turbulent Kinematics Energy for Swirl Jet subjected to VGJ at (α=0°, mr=0.095), (α=45°, mr=0.095), (α=90°, mr=0.095), (α=0°, mr=0.285), (α=45°, mr=0.285), and (α=90°, mr=0.285), are shown in figures 8.a, b, c, d, e, and f, respectively. All VGJs excited cases show higher Turbulent Kinematics Energy than the Baseline Jet. The higher VGJs momentum case mr=0.285 exhibits higher Turbulent Kinematics Energy than the cases of mr=0.078 and 0.095. The momentum ratio 0.285 is equivalent to CR equal unity. With excitation the high stress region located at a cylinder layer of diameter 0.8 of nozzle diameter and moving horizontally in a section from 2 to 3 z/D from upstream according to momentum ratio.

4- CONCLUSIONS

The use of Vortex Generator Jets to enhance the mixing between a turbulent jet and the surrounding fluid was shown to offer improvement and control over the jet evolution.

- The Swirl has higher Turbulent Kinematics Energy than the baseline jet. The VGJs increased and spreaded the turbulent kinetic energy in the main (swirl) jet.
- The Swirl Jet with injection (α=45) and the higher momentum injection gives maximum higher Turbulent Kinematics Energy than the Baseline Jet by 18.5, 29.4, 38.7 or 122.6% for mr equals 0.055, 0.078, 0.095 or 0.285 respectively.
- Tangential VGJs injection does not similar to experimental results since the experimental results does not allow ideal tangentional injection (Non-radial component) because it have $\pm$ 8 degrees deviation due to the diameter of VGJ,
- Further downstream, a wide range of turbulence structures associated with the VGJs injection affect the velocity fluctuations and enhance mixing between turbulent jet and surrounding fluid.
- With Swirl Jet excitation the high stress region located at a cylinder layer of diameter 0.8 of nozzle diameter and moving horizontally in a section from 2 to 3 z/D from upstream according to momentum ratio.

5- REFERENCES

CFDRC, 2000, "CFD-ACE+ Theory and Users' Manuals Ver.6.4" *CFD Research Corporation*, Huntisville, Al., USA.

Corke, T. C. and Kusek S. M., 1993, "Resonance in Axisymmetric Jets With Controlled Helical-Mode Input" *Journal of Fluid Mechanics*, Cambridge University Press, Vol. 249, pp. 307-336.

Husain, H.S. and Hussain, F., 1993, "Elliptic Jets. Part 3. Dynamics of Preferred Mode Coherrts Structure", *Journal of Fluid Mechanics*, Vol. 248, PP. 315-361.

Longmire, E. K., Eaton J. K. and Elkins, C. J., 1992, "Control of Jet Structure by Crown-Shaped Nozzles," *AIAA Journal*, Vol. 30, No. 2, pp. 505-512.

Martin, J. E. and Meiburg, E., 1991, "Numerical Investigation of Three-Dimensionally Evolving Jets Subjected to Axisymmetric and Azimuthal Perturbations," *J. Fluid Mech.*, Vol. 230, pp. 271-318.

Mostafa, N. H., Rediniotis, O.K. and Vandsburger, U., 1995, "Flow Field Characteristics of Circular Swirl Jet Generated by Vortex Generating Jets", *ASME Fluids Engineering Division Summer Meeting, High Speed Jet Flows Forum*, PP.89-95. Hilton Head Island, South Carolina.

Mostafa, N. H., Vandsburger, U., and Economides, T.A., 1996, "Flow Field Characteristics of a Turbulent Round Jet Subjected to Pulsed Vortex Generating Jets" *ASME Fluids Engineering Division Summer Meeting . High Speed Jet Flows Forum*, FED-Vol. 237, PP. 535-542, San Diego, CA.

Mostafa, N. H. and Vandsburger, U., 1998, "The Visible Structure of Turbulent Jet Flames Subjected to Vortex Generating jets" *ASME Fluids Engineering Division Summer Meeting, High Speed Jet Flows Forum*, Washington D.C., USA, June 21-25.

Mostafa, N. H., Le-Pera, S. and Vandsburger, U., 1999, - "Evaluation of Turbulence Scales in a Jet Subjected to Vortex Generating Jets" " N. H. *Forum on High speed Jet Flows, the3rd ASME/JSME Joint Fluids Engineering Conference*, San Francisco, CA.

Mostafa, N. H., 2000, "Space/Time Variation of Energy in the Jet Subjected To Vortex Generating Jets" *Forum on High speed Jet Flows VI, ASME Fluids Engineering Conference*, Boston, Massachusetts, USA.

Parekh, D.E., Kibeus V., Glezer, A., Wiltze, J.M., and Smith, 1996, "Innovative Jet Flow Control: Mixing Enhancement Experiments, " *AIAA 96-0308.*

Raman G. and Cornelius D., 1995, "Jet Mixing Control Using Excitation From Miniature Oscillation Jets," *AIAA Journal*, Vol.33, No 2, pp 365-368.

Sighal, A. K. "Key elements of verification and validation of CFD software" *AIAA98-2639, 29th* AIAA, Fluid dynamic conference, Allbuqurqe, NM, June 15-18, 1998.

Vandsburger, U. and Ding, C. ,1995, "The Spatial Modulation of a Forced Triangular Jet" *Journal Experiments in Fluid.* Vol. 18, PP 239-248.

Wiltse, J. M. and Glezer, A., 1993, "Manipulation of Free Sheer Flows Using Piezoelectric Actuators" *Journal Fluid Mechanic*, Vol. 249, pp. 261-285.

Zaman, K. B. M. Q. a, Reader, M. F and Samimy, M., 1994, "Control of an Axisymmetric Jet Vortex Generators," *J. Phys. Fluid* Vol. 6, No. 2, pp. 778-793.

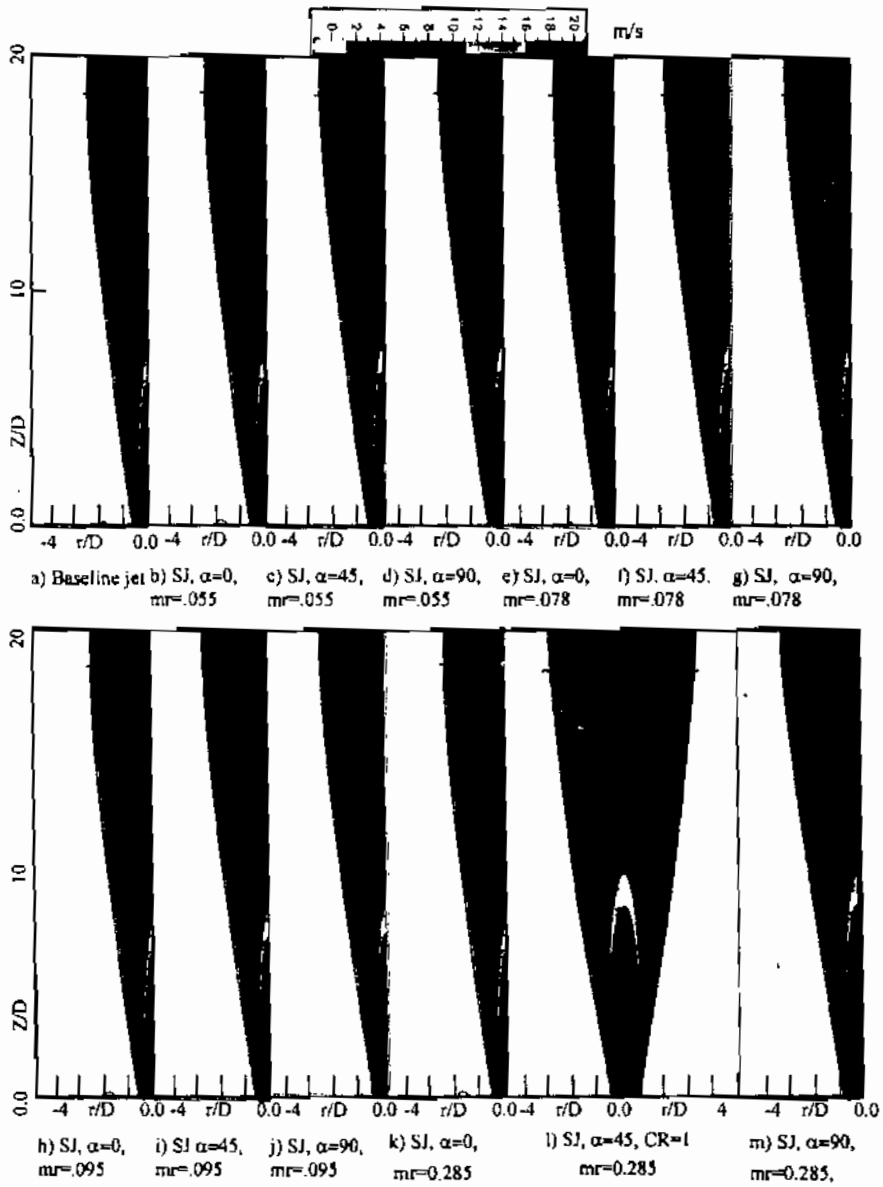

Fig. (2) Iso-contour of (U) for baseline jet and Swirl Jet across diametric plane.

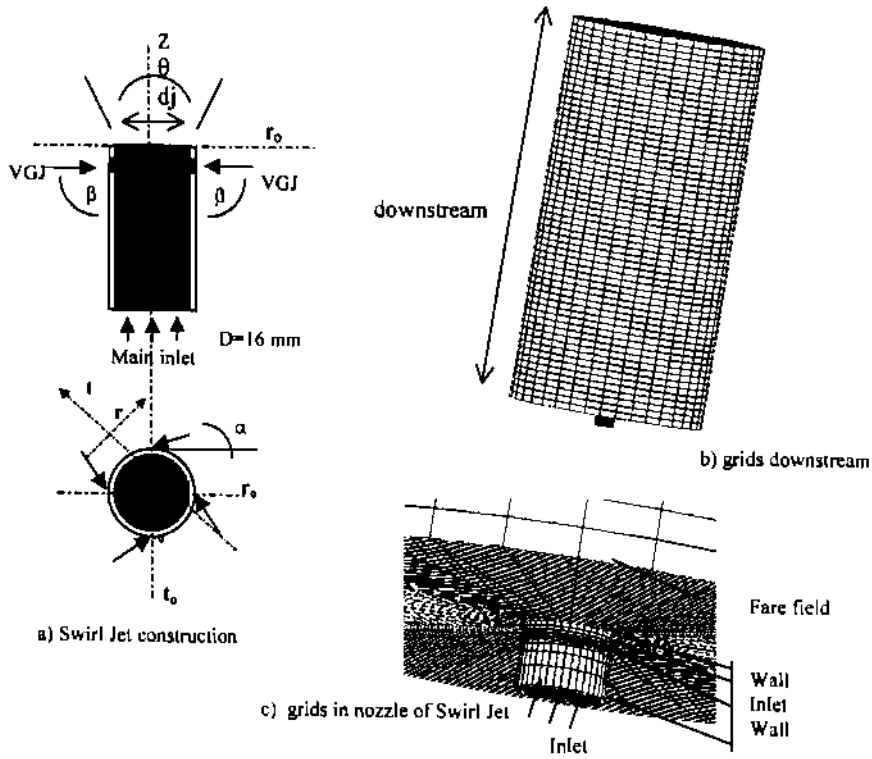

Fig (1) grids in Swirl Jet and its downstream.

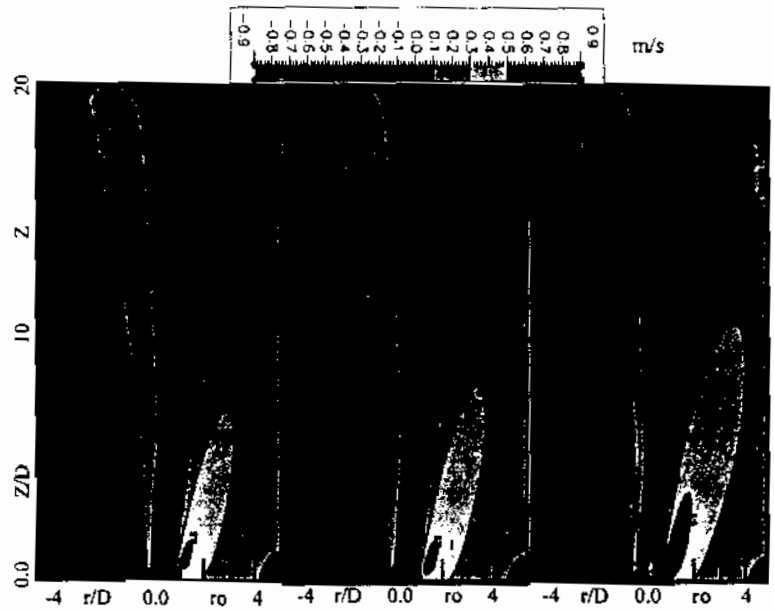

a) Baseline jet b) SJ α=45, mr=.055 c) SJ α=45, mr=0.285

Fig. (3) Iso-contour of horizontal velocity component in r_0-axis direction for baseline jet and Swirl Jet across diametric plane.

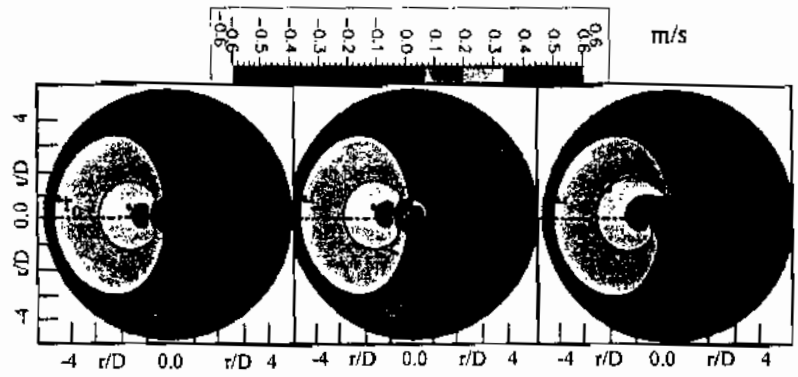

a) Baseline jet b) SJ α=45, mr=.055 c) SJ α=45, mr=0.285

Fig. (4) Iso-contour of horizontal velocity component in t_0-axis direction for baseline jet and Swirl Jet across diametric plane.

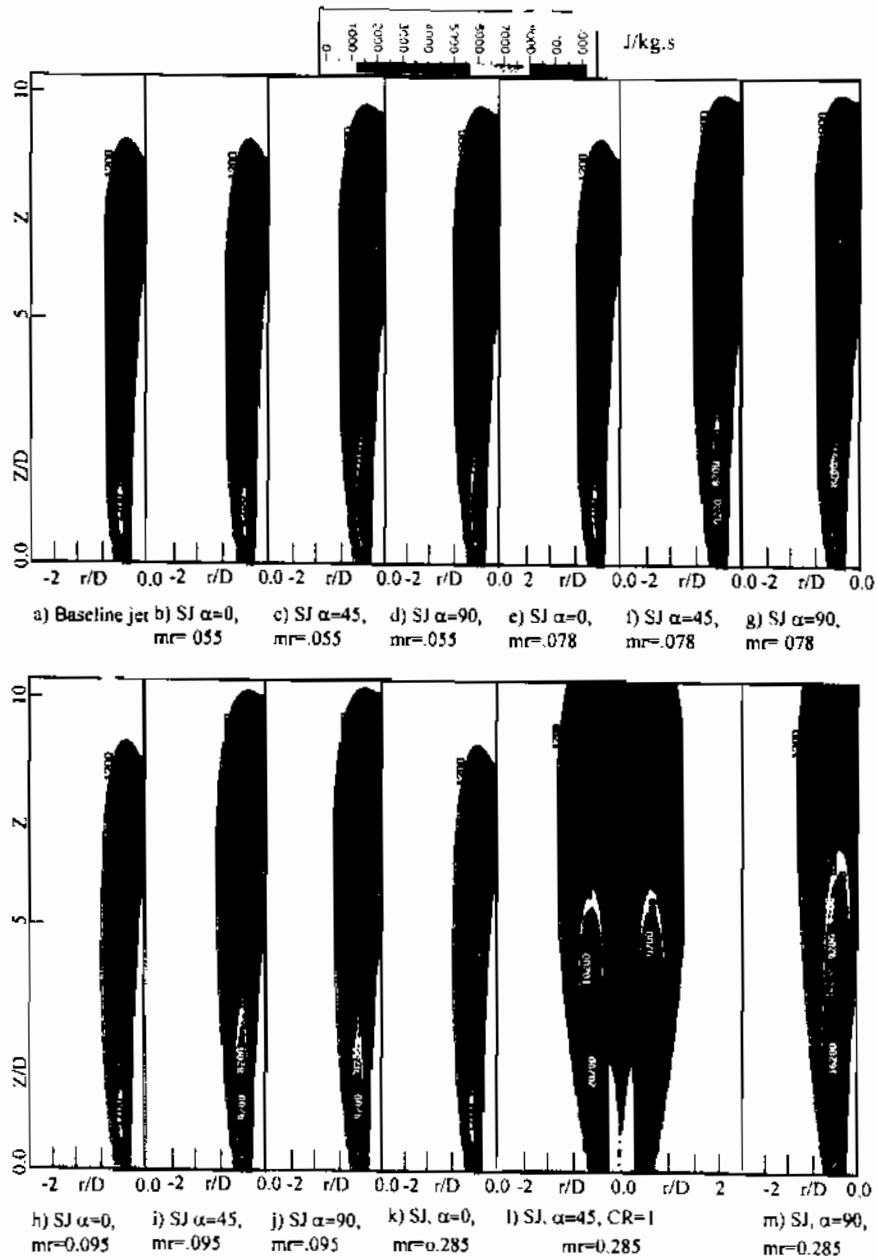

Fig. (5) Iso-contour of turbulence dissipation rate (ε) for baseline jet and Swirl Jet across diametric plane.

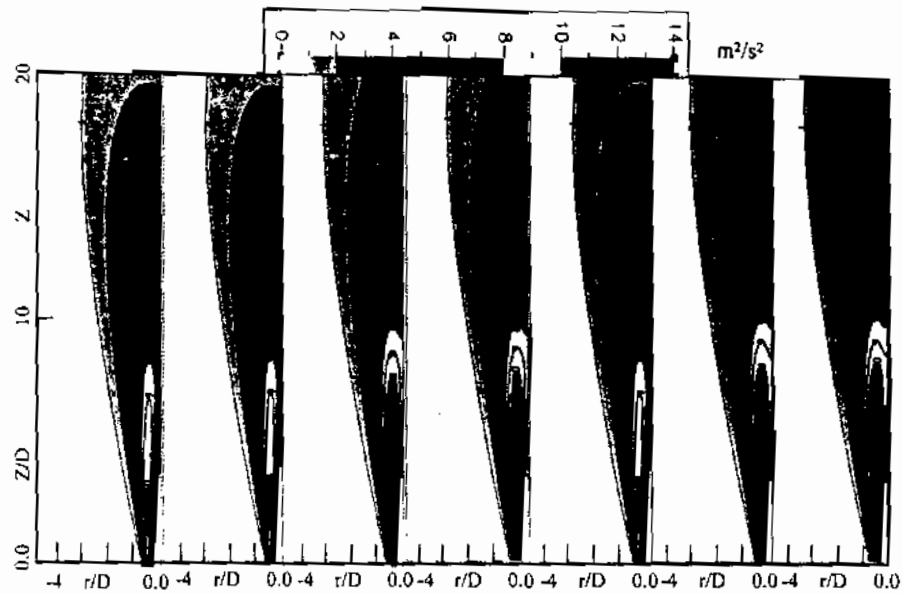

a) Baseline jet b) SJ, α=0, mr=.055 c) SJ, α=45, mr=.055 d) SJ, α=90, mr=.055 e) SJ, α=0, mr=.078 f) SJ, α=45, mr=.078 g) SJ, α=90, mr=.078

Fig. (6) Iso-contour of turbulent kinetic energy (k) for baseline jet and Swirl Jet across diametric plane.

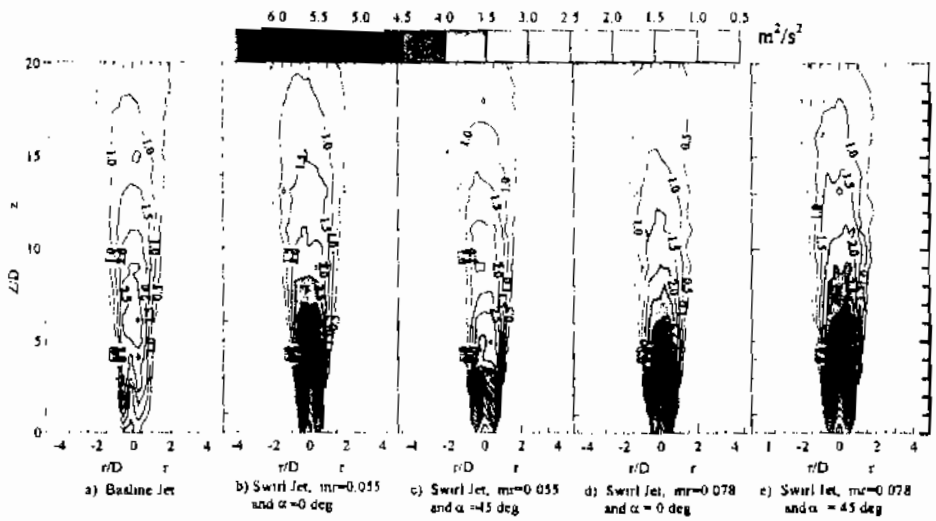

Fig. (7) Iso-contour of total turbulence energy ($U'^2+V'^2+W'^2$) for Baseline Jet and Swirl Jet across diametric plane, Mostafa (2000).

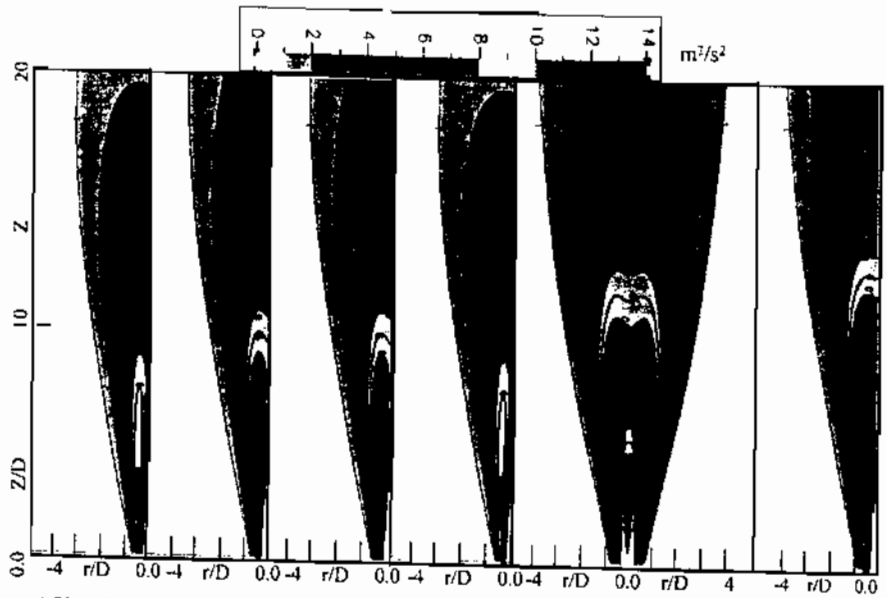

a) SJ, α=0, mr=.095 b) SJ, α=45, mr=.095 c) SJ, α=90, mr=.095 d) SJ, α=0, mr=0.285 e) SJ, α=45, CR=1 mr=0.285 f) SJ, α=90, mr=0.285

Fig. (8) Iso-contour of turbulent kinetic energy (k) for Swirl Jet across diametric plane.